

INTERNAL MODEL CONTROL OF A PHYSICAL VAPOR DEPOSITION EFFUSION SOURCE

S. Tobias Junker ^{*,***}, Robert W. Birkmire ^{**,***},
Francis J. Doyle III ^{****}

** Department of Chemical Engineering*

*** Institute of Energy Conversion*

**** University of Delaware, Newark, DE 19716, USA*

***** Department of Chemical Engineering,
University of California, Santa Barbara, CA 93106, USA*

Abstract: Internal model based temperature controllers are developed for effusion sources that are part of a continuous process for production of thin-film photovoltaic modules. Operation of this system in a research framework necessitates the ability to perform fast, overshoot-free reference changes. To address input constraints, controllers are implemented using an anti-windup scheme. Both empirical ARMAX models and a simplified fundamental model are utilized. Controllers were designed in simulation studies and tested in experiments and a very good match between simulation and experiment was obtained.

Keywords: solar cells, ARMAX models, dynamic models, control oriented models, model based control

1. INTRODUCTION

The effusion sources are part of a continuous process for production of thin-film photovoltaic modules. The approach considered in the present work is the manufacture of Copper-Indium-Gallium-Diselenide (CIGS) films by deposition onto a flexible substrate using a roll-to-roll processing scheme (Birkmire and Eser, 1997). The film is deposited by thermal evaporation from a series of elemental sources located sequentially through the deposition zone.

A critical issue in commercializing this approach is to keep composition and thickness of the CIGS film at their setpoint over long deposition times. Due to long start-up and shutdown times, it is equally important to efficiently perform setpoint changes such that multiple recipes can be tested in a single experiment.

1.1 Process Model and Control Structure

The process can be divided into two subsystems: (1) the effusion subsystem, and (2) the deposition subsystem.

The effusion subsystem consists of the elemental sources where electric energy to resistive heaters is supplied as the input and the outputs are temperature and absorbance measured by thermocouples and atomic absorption spectroscopy sensors for

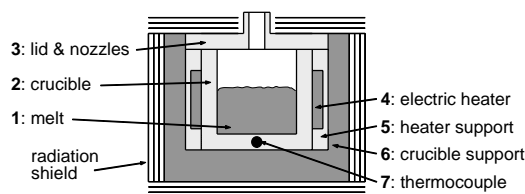


Fig. 1. Schematic cross section of effusion cell.

each source. Each effusion cell (see schematic in Figure 1) is resistively heated in order to first melt and then evaporate the metal. The crucible is covered by a lid with two nozzles. Junker *et al.* (2003) developed a fundamental mass- and heat transfer model of the effusion sources.

The deposition subsystem consists of the moving substrate to which the elemental vapor fluxes are delivered as the input and the outputs are the final film thickness and composition measured by X-ray fluorescence (Junker *et al.*, 2004).

A characteristic difference between these subsystems is their dynamic behavior. The effusion subsystem has a time delay on the order of seconds and thus reacts quickly to input changes. The deposition subsystem, on the other hand, has a long time delay on the order of several minutes.

Since the effusion subsystem's output is the deposition subsystem's input, disturbances of the former affect the latter. Based on this disturbance structure, the process should be controlled by a cascade structure where the outer control loop regulates the deposition process by providing flowrate/temperature setpoints to the inner control loop that regulates the effusion process.

For the outer loop, Junker *et al.* (2004) discuss the application of internal model control and model predictive control. For the inner loop, the present work discusses efficient internal model control for reference tracking of the copper source's temperature. The developed controllers are based on (1) a simplified form of the fundamental model, and (2) empirical models identified based on input/output data. Empirical models are developed to provide a basis of comparison for the fundamental model based controller.

1.2 Overview

The paper is organized in four main sections: development of (1) empirical ARMAX and (2) simplified fundamental models that are suitable for controller design, (3) introduction to the internal model control framework including the utilized anti-windup scheme, and (4) discussion of the obtained reference tracking results and comparison to the corresponding simulations.

2. EMPIRICAL ARMAX MODEL

A standard model structure for system description and control is the ARMAX model (Ljung, 1999, p. 83). It is a time-invariant parametric input-output model that describes the current output $y(k)$ as a function of past outputs, past inputs $u(k)$, and an estimate of the disturbance via modeling of the error $e(k)$.

2.1 Model Structure

The general model structure is given by the difference equation (Ljung, 1999, p. 83)

$$A(q)y(k) = B(q)u(k - n_k) + C(q)e(k) \quad (1)$$

where $e(k)$ is assumed to be white noise and the transfer operators A , B , and C are defined as

$$A(q) = 1 + a_1q^{-1} + \dots + a_{n_a}q^{-n_a} \quad (2)$$

$$B(q) = b_1 + \dots + b_{n_b}q^{-(n_b-1)} \quad (3)$$

$$C(q) = 1 + c_1q^{-1} + \dots + c_{n_c}q^{-n_c} \quad (4)$$

where q^{-1} is a backward shift operator, i.e.,

$$u(k - 1) = u(k) \cdot q^{-1} \quad (5)$$

and the model order is defined by the integers (n_a, n_b, n_c, n_k) . Here, n_a is the number of poles, $(n_b - 1)$ the number of zeros, and n_k the time delay. Different model structures are identified by the notation **ARMAX** _{n_a, n_b, n_c, n_k} .

2.2 Experiment Design

Empirical system identification (ID) of ARMAX models is based on I/O data collected from the process to be modeled. Since the true system is nonlinear the experiment should be carried out at the nominal operating point and the input data should be "rich", i.e., excite the system and force it to show its properties (Ljung, 1999, p. 411).

A common input sequence is a random binary sequence that randomly switches the input between two values u_1 and u_2 . The minimum switching frequency must neither be too fast to allow the process to react nor too slow to prevent getting a series of step responses. For the effusion source, a value of $n_{\min} = 4$ samples at a sampling time of $T_s = 2$ seconds gives good results.

A random binary sequence at the operating point is implemented in two stages: (1) the process is driven to the setpoint via PID control and the control move u^* required to sustain this setpoint is noted, (2) the upper and lower limits are chosen as a 10% variation of u^* , i.e., $u_{1,2} = (1 \pm 0.1)u^*$.

2.3 Model Estimation

Model estimation and analysis is carried via routines from MATLAB's system identification toolbox (Ljung, 2002). Since the models are used for controller design, proper prediction of the dynamic (high frequency) behavior is crucial. This is more important than the absolute values (low frequency) since incorrect absolute values are more easily compensated for by the controller.

In addition, the residuals should be independent of the input and of each other (Ljung, 2002, p. 2-32). This is tested via the cross-correlation and auto-correlation functions, respectively, that should lie entirely within their 99% confidence intervals for the validation data set.

2.4 Results

Based on an old data set, an ARMAX_{2,1,6,2} model was identified (see Table 1, left); a comparison of experimental and predicted data is shown in Figure 2. The residuals (not shown) lie almost entirely within their 99% confidence intervals, however, the dynamic behavior is not very well predicted.

Table 1. ARMAX model parameters.

ARMAX _{2,1,6,2}		ARMAX _{4,1,1,10}	
Coefficient	Value	Coefficient	Value
a_1	-1.9705	a_1	-1.9482
a_2	$9.7059 \cdot 10^{-1}$	a_2	$7.9386 \cdot 10^{-1}$
b_1	$1.3123 \cdot 10^{-3}$	a_3	$2.8465 \cdot 10^{-1}$
c_1	$-3.4350 \cdot 10^{-1}$	a_4	$-1.3019 \cdot 10^{-1}$
c_2	$-1.9255 \cdot 10^{-1}$	b_1	$9.3174 \cdot 10^{-4}$
c_3	$-3.7459 \cdot 10^{-1}$	c_1	$-9.6967 \cdot 10^{-1}$
c_4	$-1.3116 \cdot 10^{-1}$		
c_5	$7.9861 \cdot 10^{-2}$		
c_6	$4.0042 \cdot 10^{-2}$		

For comparison, an ARMAX_{4,1,1,10} model was identified based on a more recent data set (see Table 1, right); experimental and predicted data are shown in Figure 3. Unlike the previous model, a separate validation data set was available and the shown results use this data set. Clearly, the results are very good since the dynamic behavior is very well captured and since the residuals (not shown) lie entirely within their 99% confidence interval.

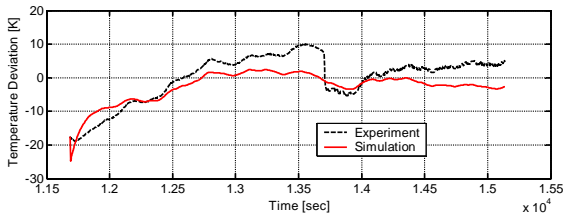


Fig. 2. Simulation of ARMAX_{2,1,6,2} model.

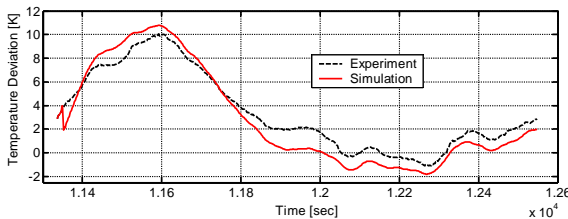


Fig. 3. Simulation of ARMAX_{4,1,1,10} model.

3. SIMPLIFIED FUNDAMENTAL MODEL

The fundamental model developed by Junker *et al.* (2003) is a set of nine coupled nonlinear ordinary differential equations. Since this form is not suitable for internal model control design, simple first and second order plus time delay models are determined based on a simulated process reaction curve. This is preferred to a Taylor linearization since the low model orders simplify controller design. It is justified *a posteriori* since the controllers perform equally well as those based on the more detailed ARMAX models developed in the previous section.

The models' transfer functions are given by

$$M_1 = \frac{K_1 e^{-\alpha_1 s}}{\tau_{1,1} s + 1} \quad (6)$$

$$M_2 = \frac{K_2 e^{-\alpha_2 s}}{(\tau_{2,1} s + 1)(\tau_{2,2} s + 1)} \quad (7)$$

where the first index refers to the model order. The gain K is computed directly as the quotient of final process output and input step size while time constants τ and time delay α are computed via a least-squares optimization that minimizes the sum-squared error between step response and prediction (see Table 2).

Table 2. Parameters of first and second order plus time delay models.

K_1 [$\frac{^\circ\text{C}}{\% \text{power}}$]	α_1 [s]	$\tau_{1,1}$ [s]	K_2 [$\frac{^\circ\text{C}}{\% \text{power}}$]	α_2 [s]	$\tau_{2,1}$ [s]	$\tau_{2,2}$ [s]
8.19	78.16	539.96	8.19	17.64	527.23	69.88

The normalized residuals are shown in Figure 4. Consistent with intuition, the second order plus time delay (SOPTD) model is a better representation the process's high frequency character. Therefore, controllers are designed based on this model only.

4. INTERNAL MODEL CONTROL

4.1 Basic Structure

Internal model control (IMC) is characterized by two main features (see Figure 5): (1) the output

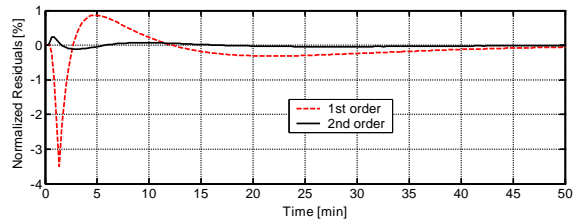


Fig. 4. Residuals of first and second order plus time delay models.

y of process P is compared to the output \hat{y} of model M in order to obtain an estimate of the unmeasured disturbance d , and (2) the controller C is designed from an inverse of the process model (Garcia and Morari, 1982).

Model invertibility is limited by time delays and right half plane zeros. If contained in the model, it has to be factorized into an invertible part M_- and a noninvertible part M_+ (Garcia and Morari, 1982). The controller is then given by

$$C = \frac{F}{M_-} \quad (8)$$

where F is an appropriately chosen filter (Morari and Zafriou, 1989; Ogunnaike and Ray, 1994). A typical n^{th} order filter is

$$F = \frac{1}{(\lambda s + 1)^n} \quad (9)$$

where λ is the tuning parameter — a larger λ leads to more sluggish control action.

4.2 Anti-windup Design

Control of the effusion source is limited by actuator constraints since the electric heater has a maximum power output of 2kW. Without proper compensation, this results in very sluggish control since the controller is unaware of the input saturation.

The situation can be remedied by using the anti-windup framework of Zheng *et al.* (1994). The basic idea is to minimize the difference between the unconstrained and constrained process outputs by introducing an additional feedback loop around the nonlinear saturation block (see Figure 6).

5. CONTROL RESULTS

Anti-windup IMC results are presented for empirical models based on two ID experiments and three

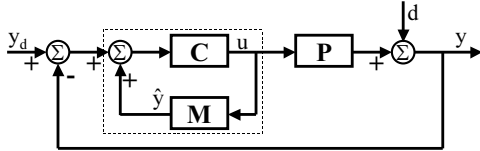


Fig. 5. Re-routed IMC structure.

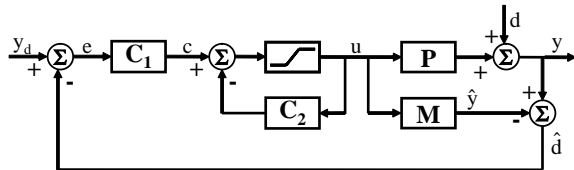


Fig. 6. Anti-windup IMC structure.

ARMAX models and for the simplified SOPTD model. For each model, a sluggish and an aggressive tuning are tested, in order to demonstrate the dependence of controller performance and noise sensitivity on the tuning. Proper controller tuning is tested in simulation studies before performing any experiments.

5.1 Empirical Model

ARMAX_{2,1,6,2} Model The results for a sluggish ($\lambda = 50s$) and an aggressive ($\lambda = 10s$) tuning are shown in Figures 7 and 8, respectively. Clearly, the simulated results are not in very good agreement with the experimental data. For the sluggish tuning, the controller is more sluggish than predicted in the tuning experiment, for the aggressive tuning, it is more aggressive and very oscillatory. These results are contradicting each other. The controller should either be always too aggressive or always too sluggish.

Since the used model is based on old data, the observed behavior is most likely caused by changes made to the experimental system between the ID and control experiments. The achieved control

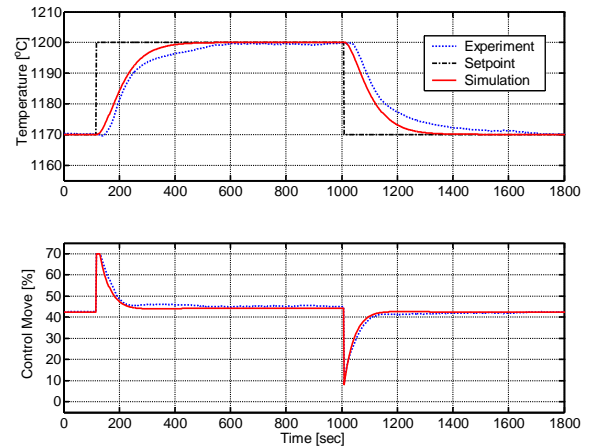


Fig. 7. ARMAX_{2,1,6,2} model with $\lambda = 50s$.

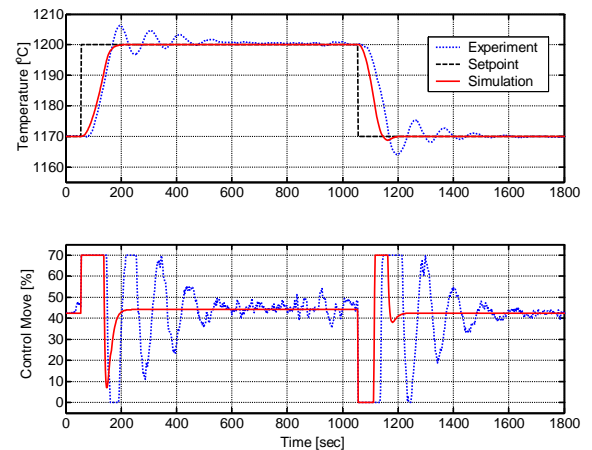


Fig. 8. ARMAX_{2,1,6,2} model with $\lambda = 10s$.

action is unacceptable such that the model in its current form is of limited value for controller design.

ARMAX_{4,1,1,10} Model Being based on a more recent ID experiment, the model's main difference besides higher n_a and n_c is a five fold increase of n_k from 1 to 5. At $T_s = 2s$, this closely matches the $\alpha = 25s$ delay of the fundamental model (Junker *et al.*, 2003).

The results for a sluggish ($\lambda = 100s$) and an aggressive ($\lambda = 22s$) tuning are shown in Figures 9 and 10, respectively. In the simulations, the experimentally observed noise was approximated by bandlimited white noise with a power of $5 \cdot 10^{-6}$ and a frequency of 50 Hz.

Unlike the ARMAX_{2,1,6,2} model, the new model is very sensitive to measurement noise. This sensitivity increases as λ decreases. For $\lambda = 22s$ this clearly has a negative effect on the output which overshoots resulting in unacceptable performance. For $\lambda = 100s$ the noise amplification is acceptable

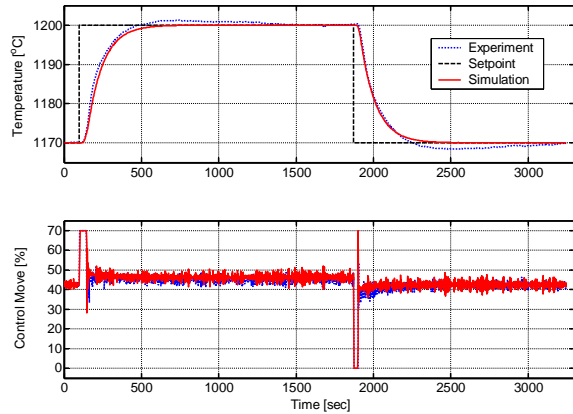


Fig. 9. ARMAX_{4,1,1,10} model with $\lambda = 100s$. Simulation with bandlimited white noise (power = $5 \cdot 10^{-6}$ @ 50 Hz).

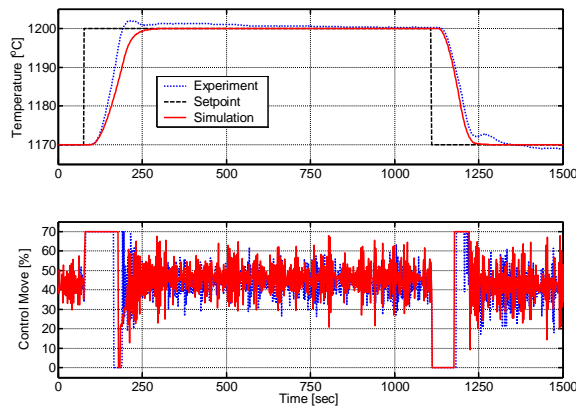


Fig. 10. ARMAX_{4,1,1,10} model with $\lambda = 22s$. Simulation with bandlimited white noise (power = $5 \cdot 10^{-6}$ @ 50 Hz).

and the simulation is in good agreement with the experiment.

Analysis The results obtained this far indicate that reference changes in less than three minutes are possible. Since neither of the two models suffices, a new model is devised by compounding the noise insensitive dynamic part (n_a, n_b, n_c) of ARMAX_{2,1,6,2} and the time delay n_k of ARMAX_{4,1,1,10} to a new ARMAX_{2,1,6,2+8} model. Applicability of this new model was verified by reproducing the ARMAX_{2,1,6,2} results in a simulation study.

5.1.1. ARMAX_{2,1,6,2+8} Model Using the same tuning constants as for ARMAX_{2,1,6,2} the results are shown in Figures 11 and 12. Both experiments show an improved performance and are closer to the simulation results.

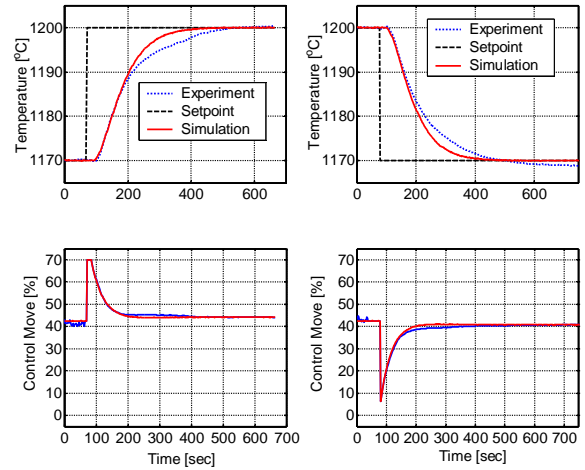


Fig. 11. ARMAX_{2,1,6,2+8} model with $\lambda = 50s$. Simulation with bandlimited white noise (power = $5 \cdot 10^{-6}$ @ 50 Hz).

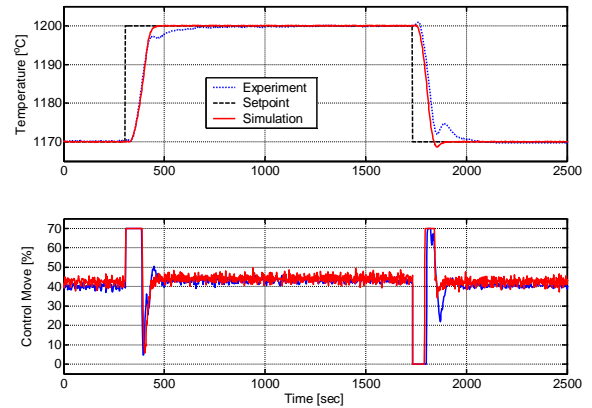


Fig. 12. ARMAX_{2,1,6,2+8} model with $\lambda = 10s$. Simulation with bandlimited white noise (power = $5 \cdot 10^{-6}$ @ 50 Hz).

5.2 SOPTD Model

For the simplified fundamental model, the tuning constant λ is defined with respect to the model time constants via the dimensionless tuning constant L , i.e.,

$$\lambda = L \cdot \frac{\tau_{2,1} + \tau_{2,2}}{2} \quad (10)$$

The results for a sluggish ($L = 0.25$) and an aggressive ($L = 0.1$) tuning are shown in Figures 13 and 14, respectively. The experimental studies were performed in a single run, first for the sluggish, then for the aggressive tuning.

During the first reference change (Figure 13, left), the agreement between model and simulation is excellent. For following reference changes, there is a slight offset in the control move, however, the dynamic behavior of the control moves matches very closely.

The experimental reference changes exhibit a slight overshoot which the controller is not able to compensate for in a timely fashion. A similar overshoot can be reproduced when introducing plant model mismatch in the simulation studies, such that this is the most likely cause for the observed behavior.

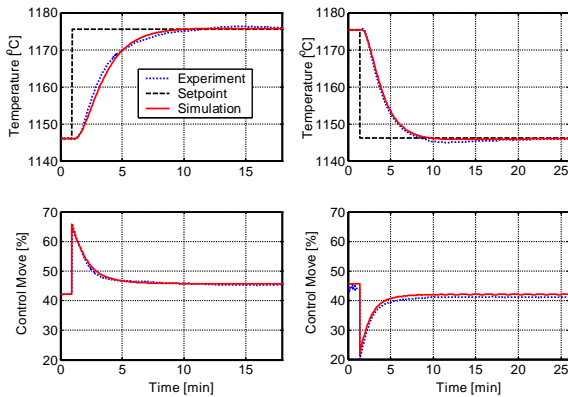


Fig. 13. SOPTD model with $\lambda = 74.64s$.

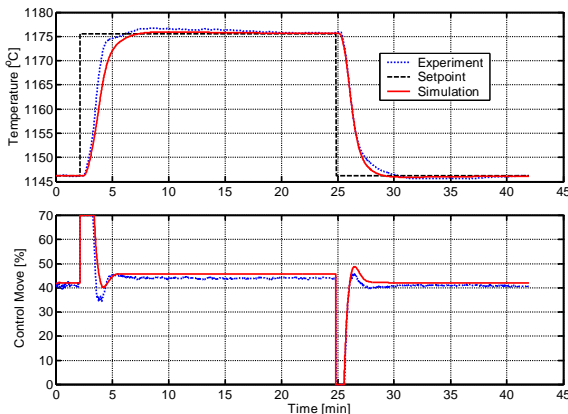


Fig. 14. SOPTD model with $\lambda = 29.86s$.

Overall, the experimental validation shows an excellent agreement with the simulation which proves the usefulness of the developed models for *a priori* controller tuning. Results obtained with the simple SOPTD model compare very favorably with the more complicated ARMAX models.

6. SUMMARY

In this paper, anti-windup internal model controllers for temperature control of a physical vapor deposition effusion source were presented. The controllers are based on both empirical ARMAX models and a simplified fundamental model. Controllers were designed in simulation studies and tested in experiments. A very good match between simulation and experiment was obtained which proves the usefulness of the developed models for *a priori* controller tuning. Controllers based on both models achieved good performance for fast, overshoot-free reference tracking.

ACKNOWLEDGEMENTS

Funding from *Global Solar Energy* and the *Delaware Research Partnership* is gratefully acknowledged.

REFERENCES

- Birkmire, R.W. and E. Eser (1997). Polycrystalline thin film solar cells: Present status and future potential. *Annu. Rev. Mater. Sci.* **27**, 625–653.
- Garcia, C.E. and M. Morari (1982). Internal model control - 1. Unifying review and some new results. *Ind. Eng. Chem. Proc. DD* **21**(2), 308–323.
- Junker, S.T., R.W. Birkmire and F.J. Doyle III (2003). Mass- and heat transfer modeling of a physical vapor deposition effusion source. *AIChE J.*, **submitted**.
- Junker, S.T., R.W. Birkmire and F.J. Doyle III (2004). Manufacture of thin-film solar cells: Modeling and control of Cu(InGa)Se₂ physical vapor deposition onto a moving substrate. *Ind. Eng. Chem. Res.* **43**(2), 566–576.
- Ljung, L. (1999). *System Identification: Theory for the User*. 2nd ed.. Prentice-Hall, Englewood Cliffs NJ.
- Ljung, L. (2002). *System Identification Toolbox, User's Guide Version 5*. The MathWorks, Inc.
- Morari, M. and E. Zafriou (1989). *Robust Process Control*. Prentice-Hall, Englewood Cliffs NJ.
- Ogunnaike, B.A. and W.H. Ray (1994). *Process Dynamics, Modeling, and Control*. Oxford University Press, New York.
- Zheng, A., M.V. Kothare and M. Morari (1994). Anti-windup design for internal model control. *Int. J. Control* **60**(5), 1015–1024.